DOI: 10.1002/zaac.200900555

Organic-Inorganic Hybrid Materials: Syntheses, X-ray Diffraction Study, and Characterisations of Manganese, Cobalt, and Copper Complexes of Modified Bis(phosphonates)

Susan Kunnas-Hiltunen,*[a] Elina Laurila,[a] Matti Haukka,[a] Jouko Vepsäläinen,[b] and Markku Ahlgrén[a]

Keywords: Bisphosphonates; Organic-inorganic hybrid composites; Manganese; Copper; Cobalt

Abstract. Four new cobalt, manganese, and copper bis(phosphonates), $[Co_2\{Cl_2C(PO_3)_2\}(H_2O)_7{\cdot}4H_2O]$ (**1**), $[Co\{Cl_2C(PO_2O(C(O)C_6H_5))_2(H_2O)_5\}{\cdot}2H_2O\{Cl_2C(PO_2O(C(O)C_6H_5))_2\}\{Co(H_2O)_6\}]$ (**2**), $[Mn\{[Cl_2C(PO_2O(C(O)C_6H_5))_2](H_2O)_3\}]$ (**3**), and $[Cu\{(CH_2C_5H_5N)C(OH)(PO_3H)_2\}_2{\cdot}4H_2O]$ (**4**), were prepared by gel, liquid, and evaporation crystallisation methods. Compounds **1**–**4** were characterised by X-ray single-crystal diffraction, elemental analysis, infrared spectroscopy, and thermogravimetric analysis. The effects of metal and various substituted groups in bis(phosphonate) ligands on the structure formation of bis(phosphonates) were studied. In the structure of **1**, the clodronic acid ligand (**L1**) is in bischelating bonding mode, and the dinuclear units of **1** are surrounded by two-dimensional water cluster patterns. The hydrogen bond network of compound **1** is extended to a three-dimensional framework when the phosphonate oxygen atoms serve as hydrogen-bond acceptors. In complex **2**, the CoO_6 octahedron shares a corner of one PCO_3 tetrahedron of the dibenzoyl derivative of clodronic acid ligand (**L2**), and forms a two-dimensional hydrogen bonding network, which consists of $[Co(H_2O)_6\}]^{2+}$ cations, lattice water molecules and **L2** ligand molecules. Compound **3**, in turn, consists of dimeric building blocks built up of PCO_3 tetrahedra of the ligand **L2**, which connect the corner-sharing MnO_6 octahedra and form an overall 2D structure through hydrogen bonds of coordinated and crystal water molecules and phosphonate oxygen atoms. Complex **4** is among the first metal complexes of risedronic acid (**L3**). In compound **4**, two **L3** ligand molecules chelate tridentately the Cu^{II} atom at the center of symmetry, and the monomeric units of **4** are connected to a 3D structure through hydrogen bonding of coordinated and lattice water molecules to both protonated and deprotonated phosphonate oxygen atoms and protonated nitrogen atoms in the pyridine ring.

Introduction

Polyfunctional ligands, for example bis(phosphonates) [alternatively named di(phosphonates)], have interesting potential properties for crystal engineering, since they are versatile building blocks. Between the phosphonate groups exists a stable organic backbone (H_2O_3P–R–PO_3H_2, R = alkyl or aryl), which is a spacer whose length and shape can be modified, and the inorganic parts have six possible donor oxygen atoms to form structure-strengthening chelate rings with metal cations [1]. In addition, the degree of protonation/deprotonation and the presence of other cations, anions, or neutral molecules in the starting mixture may have an effect on the dimensionality [2]. When, for example, Na^+ or lattice water participate in structure formation, these ions/molecules are able to connect the adjacent molecules, chains, or layers to higher dimensionalities through coordinative bonds [3] or hydrogen bonds [2a, 4], respectively. Crystal water and coordinated water may form water clusters through hydrogen bonding. These observations were widely studied both theoretically and experimentally to provide information about the bulk properties of water.

Water is a very important factor in many biological and chemical processes, and it is also important in the designing of new metal-organic framework structures [5]. Thus, the metal bis(phosphonates) are capable of forming both one-dimensional (1D) coordination polymers [2a, 6] as well as two-dimensional (2D) [7] and three-dimensional (3D) [2b–2d, 3c–3e, 4b, 4c, 7a, 8] networks. In addition, 3D microporous and mesoporous bis(phosphonate) frameworks may have chemically and thermally stabile voids or channels that can be filled by inorganic cations, anions or neutral molecules [1b, 2, 9]. Hence, metal bis(phosphonates) have versatile applications, for example, in the sorption of organic molecules and as catalysts for inorganic and organic synthesis [1]. In addition, metal phosphonates have magnetic properties at low temperatures if the metal is paramagnetic [1].

Geminal bis(phosphonates), [H_2O_3P–($R1$)C($R2$)–PO_3H_2, $R1$ = H, Cl, OH and $R2$ = Cl, CH_3, amine, alkyl chain with heterocyclic amine etc.] have a strong ability to bind metal

* S. Kunnas-Hiltunen
Fax: +358-13-251-3390
E-Mail: Susan.Kunnas-Hiltunen@joensuu.fi
[a] Department of Chemistry
University of Joensuu
P. O. Box 111
80101 Joensuu, Finland
[b] Department of Chemistry
University of Kuopio
P. O. Box 1627
70211 Kuopio, Finland

Supporting information for this article is available on the WWW under **http://dx.doi.org/10.1002/zaac.200900555** or from the author.

Zeitschrift für anorganische und allgemeine Chemie ZAAC Journal of Inorganic and General Chemistry

cations, especially calcium in hydroxyapatite crystals. This gives them an important function in the treatment of diseases affecting bone tissue and in inhibiting the mineralisation of soft tissues. The best-known drugs for the treatment of hypercalcaemia and osteoporosis are non-nitrogen-containing clodonate, e.g. disodium dichloromethylenebis(phosphonate) tetrahydrate, and nitrogen-containing risedronate, e.g. monosodium 1-hydroxy-2-(3-pyridinyl)ethylidenebis(phosphonic) acid [10]. Clodronate and its analogues are highly hydrophilic compounds, and therefore their absorption in the human body has to be improved. The hydrophilic phosphonic acid groups can be masked so that the compound formed is more hydrophobic and will release the parent clodronate after absorption by chemical and/or enzymatic hydrolysis reactions according to the prodrug principle [11]. Among the other clodronic dianhydrides, P,P'-dibenzoyl-dichloromethylenebis(phosphonate) disodium salt is the first reported bioreversible prodrug of clodronate [11a]. In addition, the hydrophobic groups can be added to the carbon bridge between the phosphonate groups, as has been done with etidronate [hydroxyethylidenebis(phosphonate)], pamidronate [3-ammonium-1-hydroxypropylidene-1,1-bis(phosphonate)] and risedronate. In risedronate, the hydroxyl group and a carbon chain, containing a nitrogen atom within a heterocyclic ring, enhance the binding to human bone [10a]. Several metal complexes of medronate [methylenebis(phosphonate)] [6a, 6b, 7b, 8a], etidronate [6c–6e, 7c–7f, 8b–8e], clodronate, and its derivatives [12] were prepared and characterised, but the number of metal complexes of this kind of modified bis(phosphonates) is very limited.

We previously reported about the alkaline earth metal [3a, 13] and the nickel and zinc complexes of the dibenzoyl derivative of clodronic acid, as well as their hydrolysis products, the nickel and zinc complexes of clodronic acid [14]. The results showed that the dibenzoyl derivative of clodronic acid can appear in various bridging and chelating modes as ligand, and it always forms 2D crystal structures with or without hydrogen bonding, even though two of the phosphonate oxygen atoms are masked with dibenzoyl groups. The clodronic acid ligand, in turn, can form a 3D hydrogen bonding network through water clusters and phosphonate oxygen atoms [14]. Our idea was to produce single crystals of bis(phosphonate) metal complexes and to study their structural properties for further research in the area of solid-state chemistry. In addition, this study provides important information in support of research into bis(phosphonates) as pharmaceutical products. Although the metals used in this study are toxic, the first row transition metal complexes are good model structures; they have similar sizes of the ionic radiuses than alkaline earth metals.

Four new manganese, cobalt, and copper bis(phosphonate) crystal structures determined by X-ray diffraction, elemental analysis, IR spectroscopy, and thermogravimetric analysis are reported in this article. The complexes were the cobalt complex of clodronic acid (**L1**) $[Co_2\{Cl_2C(PO_3)_2\}(H_2O)_7{\cdot}4H_2O]$ (**1**), the cobalt and manganese complexes of the dibenzoyl derivative of clodronic acid (**L2**) $[Co\{Cl_2C(PO_2O(C(O)C_6H_5))_2(H_2O)_5\}{\cdot}2H_2O\{Cl_2C(PO_2O(C(O)C_6H_5))_2\}\{Co(H_2O)_6\}]$ (**2**), and $[Mn\{[Cl_2C(PO_2O(C(O)C_6H_5))_2](H_2O)_3\}]$ (**3**), and the copper complex of risedronic acid (**L3**) $[Cu\{(CH_2C_5H_5N)C(OH)(PO_3H)_2\}_2{\cdot}4H_2O]$ (**4**).

Results and Discussion

Crystal Structure of $[Co_2\{Cl_2C(PO_3)_2\}(H_2O)_7{\cdot}4H_2O]$ (1)

The asymmetric unit of complex **1** consists of two independent cobalt atoms, one **L1** ligand, seven aqua ligands and four lattice water molecules. The deprotonated clodronic acid ligand **L1** has a bischelating bonding mode, where two phosphonate PCO_3 tetrahedra share corners of two CoO_6 octahedra. In addition, the CoO_6 octahedron shares corners through μ-H_2O ligand oxygen atom O6, and thus, form a cluster-like structure. The other coordination sites of the atoms Co1 and Co2 are occupied by aqua ligands (see Figure 1). The variety of the Co1–O [(Co1–O)av = 2.1095 Å] and Co2–O [(Co2–O)av = 2.1076 Å] bond lengths shows the distortion of the CoO_6 octahedron (see Table 1), where the longest Co–O bonds are between the cobalt atoms and the μ-H_2O oxygen atom. The O–Co1–O angles lie in the range of 86.0–179.1 °, and the O–Co2–O angles in a range from 85.3 to 175.6 °. The intermetallic Co1–Co2 distance amounts 3.8380(3) Å. Compound **1** is isostructural with the previously published nickel and zinc complexes of clodronic acid [16], and the *M*–O bond lengths and the O–*M*–O angles follow the same pattern. In addition, a similar bischelating bonding mode is found, for example, in the cobalt and vanadium complexes of medronate [8f, 15], copper complexes of etidronate [8c–8d], aluminium complexes of ethylenediphosphonate [16], magnesium complexes of clodronate [3a] and calcium [12a] and cadmium [12b] complexes of monoethyl, and cobalt complexes of P-piperidinium-P'-methyl [12c] derivatives of clodronate.

In the packing scheme of complex **1**, the crystal water molecules surround the inorganic parts of the dinuclear motifs, which are organised in *zig-zag* mode along the [100] plane (Figure 1). After the lattice water was removed, the space that crystal water accommodates was determined by means of the PLATON software SOLV [17] to be 158.8 $Å^3$ (9.1 % of the total unit cell volume), where as the corresponding values of the previously reported nickel and zinc complexes of clodronic acid were 286.6 $Å^3$ (16.8 %) and 460.0 $Å^3$ (23.2 %), respectively [14]. The shape of the solvent-accessible space in complex **1** is illustrated as a space-filling model in Figure 2, made with the PLATON software CAVITY [17]. Compound **1** has as many coordinated and crystal water molecules as the nickel complex of clodronic acid $[Ni_2\{Cl_2C(PO_3)_2\}(H_2O)_7{\cdot}4H_2O]$ [14]. Thus, the slightly different packing of the lattice water has an influence on the size of the space that the water molecules accommodate. In turn, the zinc complex of clodronic acid $[Zn_2\{Cl_2C(PO_3)_2\}(H_2O)_7{\cdot}6H_2O]$ has more lattice water molecules, which surround the whole dimeric zinc clodronate units [14]. In complex **1**, the solvent-accessible spaces do not penetrate the structure continuously, as in the nickel and zinc complexes, but the lattice water is blocked inside the structure.

The coordinated water molecules and the crystal water of compound **1** form infinite hydrogen-bonded tapes along the

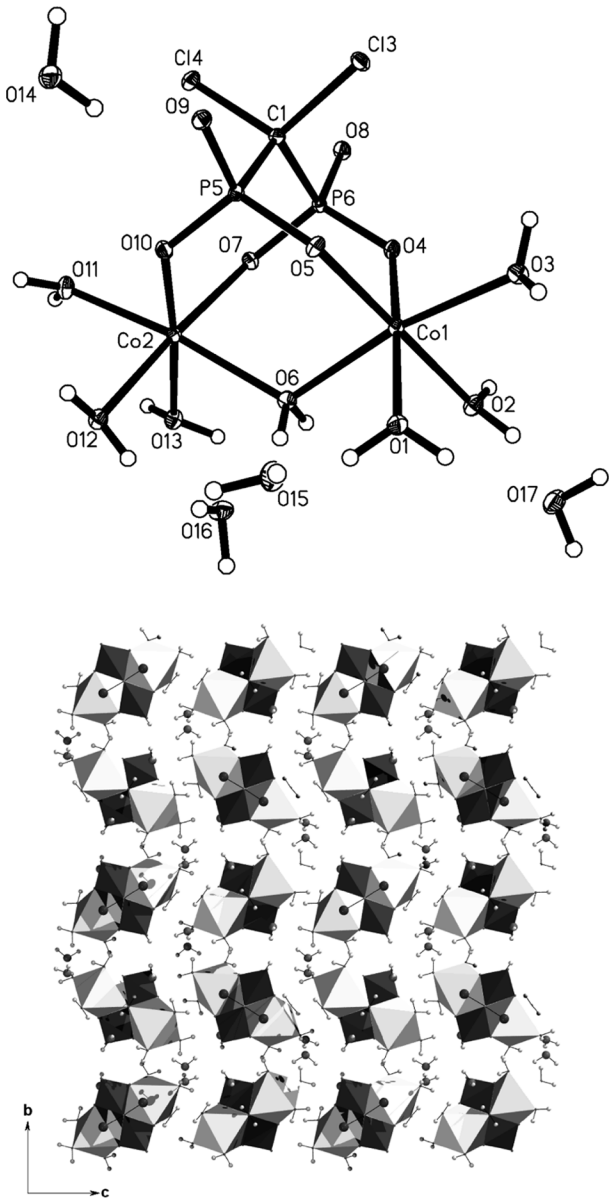

Figure 1. Molecular structure of **1** with numbering scheme and thermal ellipsoids (50 %, top image). Packing of the dinuclear motifs of **1** (bottom image, PCO_3 tetrahedron = dark grey; CoO_6 octahedron = light grey).

Table 1. Selected *M*–O bond lengths /Å and O–*M*–O angles /° for compound **1**.

1			
Co1–O5	2.0263(11)	Co2–O10	2.0311(11)
Co1–O2	2.0550(11)	Co2–O7	2.0741(11)
Co1–O4	2.0764(11)	Co2–O13	2.0818(11)
Co1–O1	2.1179(11)	Co2–O12	2.1248(11)
Co1–O3	2.1582(11)	Co2–O11	2.1327(11)
Co1–O6	2.2232(11)	Co2–O6	2.2010(11)
O5–Co1–O2	179.10(5)	O10–Co2–O7	94.06(4)
O5–Co1–O4	93.51(4)	O10–Co2–O13	174.42(5)
O2–Co1–O4	87.39(4)	O7–Co2–O13	91.33(4)
O5–Co1–O1	89.28(4)	O10–Co2–O12	85.30(4)
O2–Co1–O1	89.83(4)	O7–Co2–O12	175.58(4)
O4–Co1–O1	175.09(4)	O13–Co2–O12	89.44(4)
O5–Co1–O3	92.96(4)	O10–Co2–O11	91.27(4)
O2–Co1–O3	86.89(4)	O7–Co2–O11	94.70(4)
O4–Co1–O3	97.47(4)	O13–Co2–O11	86.82(4)
O1–Co1–O3	86.40(4)	O12–Co2–O11	89.69(4)
O5–Co1–O6	92.75(4)	O10–Co2–O6	95.32(4)
O2–Co1–O6	87.28(4)	O7–Co2–O6	88.10(4)
O4–Co1–O6	89.87(4)	O13–Co2–O6	86.33(4)
O1–Co1–O6	85.96(4)	O12–Co2–O6	87.60(4)
O3–Co1–O6	170.40(4)	O11–Co2–O6	172.65(4)

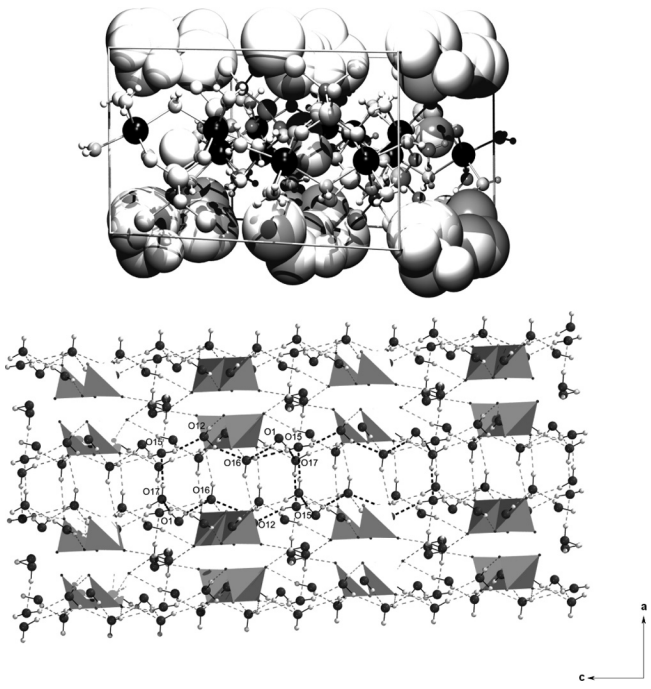

Figure 2. Space-filling illustrations of solvent accessible voids of compound **1** (top image, unoccupied space appears as white space-filling, metal atoms as black spheres, phosphorus atoms as grey spheres, chlorine atoms as grey spheres and oxygen atoms as light grey spheres). Close view of the hydrogen bonding of the water clusters in compound **1** (bottom image, PCO_3 tetrahedron = grey; oxygen atoms = dark grey; hydrogen atoms = light grey; hydrogen bond interactions = grey and black dashed lines.).

crystallographic *c* axis, where the $(H_2O)_{10}$ rings are joined together by the intramolecular O16···O15 hydrogen bonds (see the black dashed lines in Figure 2). The $(H_2O)_{10}$ ring includes the intramolecular O1···O17, O12···O16, and O1···O16, and the intermolecular O17···O15^{i}, O15···O12^{ii} hydrogen bonds with an average O···O distance of 2.813 Å and O–H···O angles of 134.1–166.1 °. The O···O distance is longer than the corresponding value of ice I_h (2.759 Å [5c]), and slightly shorter than the distance of liquid water (2.854 Å [5c]), In addition, the phosphonate oxygen atoms serve as hydrogen-bond acceptors, and the overall hydrogen bond network is three-dimensional. In addition to the above mentioned hydrogen bonds, the intramolecular O2···O17, O14···O9, O6···O16 distances lie in the range of 2.646(2)–3.115(2) Å and the angles of 134.1–160.3 °. The intermolecular O16···O8^{iii}, O12···O4^{iii}, O6···O14^{iv}, O2···O10^{iv}, O15···O8^{iii}, O17···O9^{v}, O3···O5^{v}, O13···O14^{iv},

Zeitschrift für anorganische und allgemeine Chemie ZAAC Journal of Inorganic and General Chemistry

O13···O7^{vi}, O16···O9^{vii}, O3···O15^{v}, O11···O7^{vi}, O11···O3^{iii}, and O14···O8^{viii} distances vary from 2.646(2) Å to 3.052(2) Å (symmetry code: i: –*x*, 1–*y*, –*z*; ii: *x*, 0.5–*y*, –0.5+*z*; iii: 1–*x*, –0.5+*y*, 0.5–*z*; iv: 1–*x*, 0.5+*y*, 0.5–*z*; v: 1–*x*, 1–*y*, –*z*; vi: 1–*x*, 1–*y*, 1–*z*; vii: –1+*x*, *y*, *z*; viii: 2–*x*, –0.5+*y*, 0.5–*z*); and the bond angles are in the range 145.7–172.5 °. The O16···Cl4^{vii} and O16···Cl3^{vii} distances of 3.2726(12) and 3.2860(12) Å and the O16···H16B···Cl4 and O16···H16B···Cl3 angles of 120.8 and 116.9 °, respectively, indicate intermolecular interaction between the lattice water molecule O16 and both of the chlorine atoms.

Crystal Structure of [Co{Cl$_2$C(PO$_2$O(C(O)C$_6$H$_5$))$_2$(H$_2$O)$_5$}·2H$_2$O{Cl$_2$C(PO$_2$O(C(O)C$_6$H$_5$))$_2$}{Co(H$_2$O)$_6$}] (2)

The asymmetric unit of complex **2** consists of one **L2** ligand sharing a corner of one CoO_6 octahedron through the PCO_3 tetrahedron. The coordination sphere of the cobalt ion is completed by five aqua ligands. In addition, the asymmetric unit consists of two lattice water molecules, one lattice **L2** ligand and one lattice $[Co(H_2O)_6\}]^{2+}$ cation (see Figure 3). All phosphonate oxygen atoms of the ligand **L2** and the lattice ligand **L2** are unprotonated. The distortion of the CoO_6 octahedron can be seen in the bond lengths of Co1–O [(Co1–O)av = 2.0865 Å] and Co2–O [(Co2–O)av = 2.1028 Å] (Table 2). The longest Co1–O bond lengths are between Co1 and the aqua ligand oxygen atom O10 and between Co1 and the phosphonate oxygen atom O1, respectively. The O–Co1–O angles are in the range of 84.01(8)–175.93(9) °. The $[Co(H_2O)_6\}]^{2+}$ octahedron is distorted by the Co2–O14 and Co2–O19 bonds, which are the longest bonds in the octahedron, respectively. The O–Co2–O angles range from 84.22(8)–179.28(9) °.

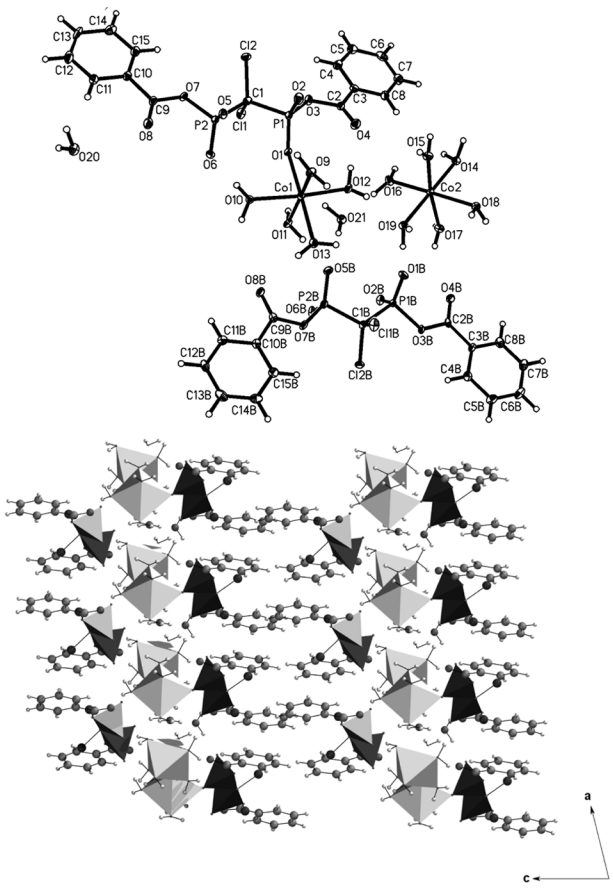

Figure 3. Molecular structure of **2** with numbering scheme and thermal ellipsoids (50 %, top image). Packing of the monomeric units of **2** (bottom image, PCO_3 tetrahedron = dark grey; PCO_3 tetrahedron of the lattice **L2** ligand = grey; CoO_6 octahedron = light grey).

The intramolecular hydrogen bonds are formed between the O17···O1B, O19···O1B, O16···O21, O10···O6, O11···O5B, O12···O19, O21···O5B, and O12···O4 atoms, with distances of 2.633(3)–2.798(3) Å and angles of 147.9–177.5 °. All monomeric units of **2** are packed facing in the same direction, one on top of the other, along the crystallographic *a* axis as a result of intermolecular hydrogen bonding between the aqua ligand, lattice water molecules and phosphonate oxygen atoms through O15···O21^{i}, O10···O18^{ii}, O15···O6^{iii} and O14···O6^{iii} with distances of 2.690(3)–2.778(3) Å and angles of 135.3–168.1 ° (Figure 3). The 2D layer-like hydrogen bond network along the [001] plane is formed through intermolecular hydrogen bonds in the direction of the crystallographic *b* axis. The intermolecular O14···O5^{iv}, O18···O2B^{i}, O13···O6B^{i}, O11···O20^{iv}, O20···O2^{ii}, O17···O10^{iv}, O19···O2B^{i}, O16···O5^{iv}, O21···O20^{iv}, O18···O8B^{iii}, O13···O4B^{v}, O9···O14^{v}, O20···O1^{v}, O9···O8B^{i}, and O19···O6B^{i} distances vary between 2.653(3) and 3.122(3) Å (symmetry code: i: 1+*x*, *y*, *z*; ii: –1+*x*, 1+*y*, *z*; iii: 1+*x*, –1+*y*, *z*; iv: *x*, –1+*y*, *z*; iiv: *x*, 1+*y*, *z*) and the angles are in the range 135.0–175.1 °. In addition, an intermolecular interaction exists between the O20 and Cl1 atoms, with a O20···Cl1^{v} distance of 3.612(2) Å and an O20···H20O···Cl1 angle of 134.9 °. As in all of the previously published metal complexes of the ligand **L2** [13, 14], the outer surfaces of the layers of complex **2** are hydrophobic due to the benzyl groups and the chlorine atoms pointing towards the interlayer section.

Crystal Structure of [Mn{[Cl$_2$C(PO$_2$O(C(O)C$_6$H$_5$))$_2$](H$_2$O)$_3$}] (3)

The asymmetric unit of complex **3** includes one independent manganese atom, one **L2** ligand and three aqua ligands (Figure 4). The **L2** ligand shares corners of two PCO_3 tetrahedra with a MnO_6 octahedron in a bidentate fashion, and forms a six-membered chelate ring. The structure of compound **3** consists of dimeric building blocks, where the **L2** ligand is also monodentately coordinated to the adjacent manganese atom (–*x*, –*y*, 1–*z*) through the PCO_3 tetrahedron, forming an eight-membered chelate ring and leaving the other phosphonate oxygen atoms deprotonated. The dimeric ring is completed by bridging of the two MnO_6 octahedra by sharing overall three corners of two PCO_3 tetrahedra (see Figure 4) through the adjacent **L2** ligand. The other coordination sites of the manganese atoms are occupied by aqua ligands, but there is no intramolecular hydrogen bonding in the structure. The Mn–O bond lengths [(Mn–O)av = 2.1815 Å] and the O–Mn–O angles (in the range of 78.3–170.4 °) show a distortion in the MnO_6 octahedron (see Table 2). The longest Mn–O bond lengths are Mn–

Table 2. Selected *M*–O bond lengths /Åand O–*M*–O angles /° for compounds **2** and **3**.

2				**3**[a)]	
Co1–O12	2.038(2)	Co2–O15	2.018(2)	Mn1–O5	2.1170(14)
Co1–O11	2.061(2)	Co2–O17	2.036(2)	Mn1–O2A	2.1231(14)
Co1–O9	2.092(2)	Co2–O16	2.050(2)	Mn1–O11	2.1793(14)
Co1–O13	2.101(2)	Co2–O18	2.153(2)	Mn1–O10	2.2108(14)
Co1–O1	2.112(2)	Co2–O19	2.173(2)	Mn1–O9	2.224(2)
Co1–O10	2.115(2)	Co2–O14	2.187(2)	Mn1–O1	2.2347(14)
O12–Co1–O11	95.01(9)	O15–Co2–O17	171.18(10)	O5–Mn1–O2A	93.29(6)
O12–Co1–O9	91.82(9)	O15–Co2–O16	95.88(9)	O5–Mn1–O11	170.44(6)
O11–Co1–O9	170.41(9)	O17–Co2–O16	92.92(9)	O2A–Mn1–O11	79.98(5)
O12–Co1–O13	91.68(8)	O15–Co2–O18	86.97(8)	O5–Mn1–O10	102.70(6)
O11–Co1–O13	84.01(8)	O17–Co2–O18	84.22(8)	O2A–Mn1–O10	161.30(6)
O9–Co1–O13	89.08(8)	O16–Co2–O18	176.96(10)	O11–Mn1–O10	85.16(5)
O12–Co1–O1	88.56(8)	O15–Co2–O19	90.82(8)	O5–Mn1–O9	87.90(6)
O11–Co1–O1	91.92(8)	O17–Co2–O19	89.84(8)	O2A–Mn1–O9	92.86(5)
O9–Co1–O1	94.98(8)	O16–Co2–O19	90.15(9)	O11–Mn1–O9	99.14(6)
O13–Co1–O1	175.93(9)	O18–Co2–O19	90.87(8)	O10–Mn1–O9	78.29(5)
O12–Co1–O10	174.90(9)	O15–Co2–O14	89.84(8)	O5–Mn1–O1	86.30(5)
O11–Co1–O10	85.33(8)	O17–Co2–O14	89.55(8)	O2A–Mn1–O1	97.80(5)
O9–Co1–O10	88.47(8)	O16–Co2–O14	89.50(8)	O11–Mn1–O1	87.89(5)
O13–Co1–O10	93.42(8)	O18–Co2–O14	89.46(8)	O10–Mn1–O1	92.89(5)
O1–Co1–O10	86.34(8)	O19–Co2–O14	179.28(9)	O9–Mn1–O1	168.13(5)

a) In structure **3**, A refers to the atom at symmetry position (–*x*, –*y*, 1–*z*).

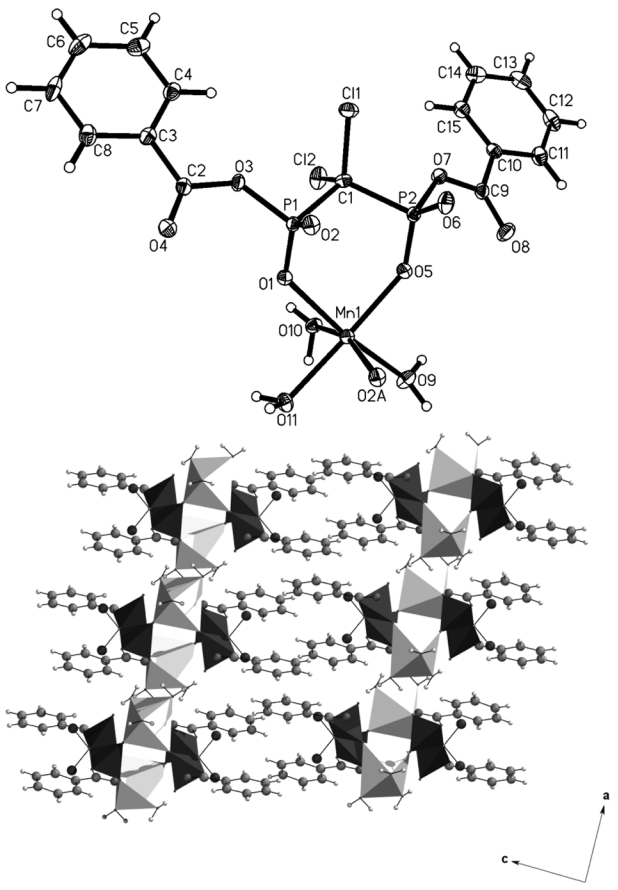

Figure 4. Molecular structure of **3** with numbering scheme and thermal ellipsoids (50 %, top image). Packing of the dimeric units of **3** (bottom image, PCO_3 tetrahedron = dark grey; MnO_6 octahedron = light grey).

O1 and Mn–O9, respectively. The dimeric units are held together by intermolecular hydrogen bonds involving all aqua ligands as donors and phosphonate and carbonyl oxygen atoms of the **L2** ligand as acceptors, forming a 2D layer-like hydrogen bond network along the [001] plane (Figure 4). The intermolecular O10···O6^{i}, O11···O1^{ii}, O11···O6^{iii}, O9···O8^{iv}, O10···O4^{ii} and O9···O4^{v} distances are in the range of 2.726(2)–3.084(2) Å (symmetry code: i: 1+*x*, *y*, *z*; ii: 1–*x*, –*y*, 1–*z*; iii: –*x*, –*y*, 1–*z*; iv: –*x*, 1–*y*, 1–*z*; v: *x*, 1+*y*, *z*) with their angles in the range 162.8–175.3 °.

Crystal Structure of $[Cu\{(CH_2C_5H_5N)C(OH)(PO_3H)_2\}_2 \cdot 4H_2O]$ (4)

Various hydrate forms of risedronate [18a, 18b] were crystallised, but among the metal complex structures, only the potassium [18c], cobalt [18d], and cadmium [18e] complexes of risedronic acid were found in literature. These metal risedronates form chains, which are further connected to a 3D structure by extensive hydrogen bonding [18c–18e]. Thus, compound **4** is among the first metal complexes of risedronate (**L3**). It consists of centrosymmetric units constructed from Cu1^{II} sharing four corners of the PCO_3 tetrahedron of two **L3** ligands. The octahedral coordination sphere of the Cu1 atom is completed with the two hydroxyl oxygen atoms of both **L3** ligands (see Figure 5). The CuO_6 octahedron is distorted by these Cu1–O7 bonds, due to the Jahn–Teller effect, resulting in a Cu1–O7 bond length of 2.656(2) Å. The Cu1–O1 and Cu1–O2 bond lengths have values of 1.944(2) and 1.9621(14) Å, respectively (Table 3). The **L3** ligand chelates the Cu1 atom tridentately, forming five- and six-membered chelate rings, with two of the four available phosphonate oxygen atoms deprotonated. The intramolecular hydrogen bond is formed between the lattice

water molecule O8 and the phosphonate oxygen atom O4, having a O8···O4 distance of 2.767(2) Å and an O8–H8O···O4 angle of 162.9 °. The intermolecular hydrogen bonds are formed in three dimensions, the protonated phosphonate oxygen atom and the pyridyl nitrogen atoms, the hydroxyl groups and the lattice water molecules serve as hydrogen-bond donors and deprotonated phosphonate oxygen atoms and lattice water molecules serve as acceptors. The intermolecular O3···O8^{i}, O6···O5^{ii}, O7···O4^{iii}, N1···O9^{iv}, O9···O1^{v}, O9···O5^{vi}, O8···O2^{iv}, and O9···O3^{vi} distances are in the range 2.555(2)–3.117(2) Å (symmetry code: i: 1–*x*, 1–*y*, –*z*; ii: –*x*, –*y*, 1–*z*; iii: 1–*x*, –*y*, –*z*; iv: 1+*x*, *y*, *z*; v: –*x*, –*y*, –*z*; vi: *x*, –1+*y*, *z*) and the angles are in the range 118.8–175.3 °. In addition, intermolecular face-to-face π–π stacking interactions exist between the adjacent pyridine rings along the crystallographic *b* axis.

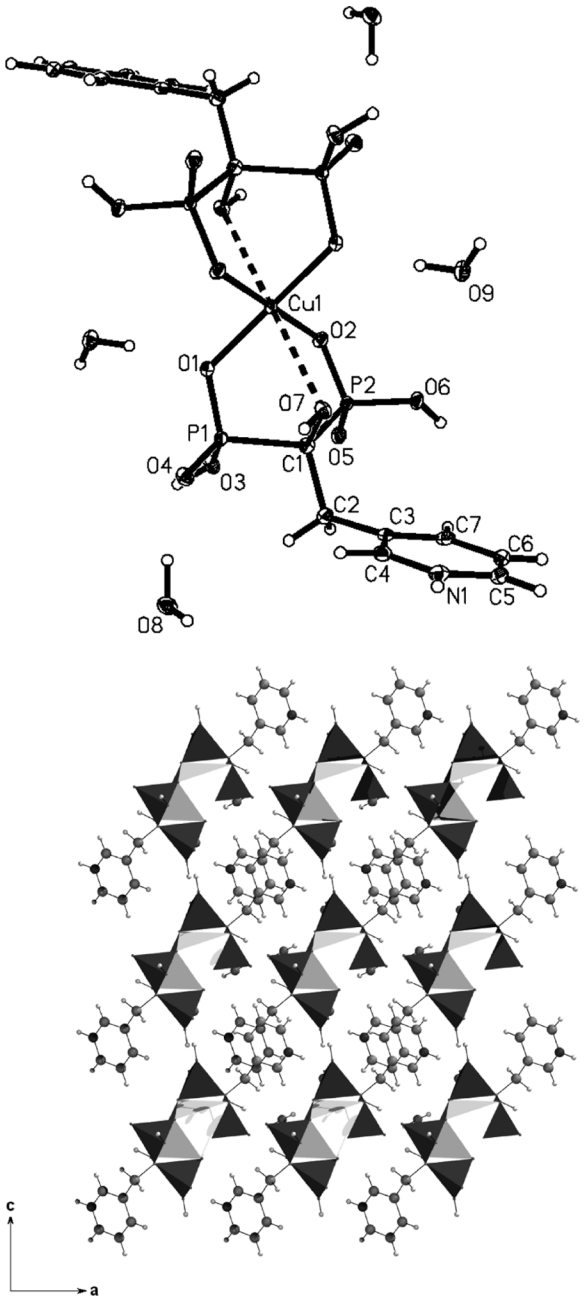

Figure 5. Molecular structure of **4** with numbering scheme and thermal ellipsoids (50 %, top image). Packing of the monomeric units of **4** (bottom image, PCO_3 tetrahedron = dark grey; CuO_6 octahedron = light grey).

Table 3. Selected *M*–O bond lengths /Å and O–*M*–O angles /° for compound **4**.

4[a)]	
Cu1–O1	1.944(2)
Cu1–O2	1.9621(14)
Cu1–O7	2.656(2)
O1–Cu1–O2	89.68(6)
O1–Cu1–O1A	180.00(8)
O2–Cu1–O2A	180.00
O1–Cu1–O7	78.12(6)
O2–Cu1–O7	77.61(5)
O1A–Cu1–O7	101.88(6)
O2A–Cu1–O7	102.39(5)
O7–Cu1–O7A	180.00(5)

a) In structure **4**, A refers to the atom at symmetry position (–*x*, –*y*, 1–*z*).

Structural Comparison

To conclude thus far, the clodronate **L1** tends to chelate and bridge metals with ionic radii of 0.74(Zn^{2+})–1.42(Ba^{2+}) Å [19] to polymeric structures, which form 2D and 3D structures through hydrogen bonding [3a, 3b, 12]. Exceptions are the monomeric strontium [12k], nickel [14] and cobalt complexes (compound **1**) of clodronic acid and dimeric zinc clodronate [14]. The isostructural nickel, zinc, and cobalt complexes form an extended 3D hydrogen-bond network. There are relatively few metal complexes from the mono ester derivatives of clodronate, but they form 2D and 3D structures, where the ethyl [12a, 12b, 12d] and phenyl ester [12a] derivatives of clodronate both chelate and bridge the metal atoms. The symmetrical diester derivatives of clodronate, in turn, both act in a chelating manner and bridge the metal atoms with ionic radii of 0.74–1.42 Å [19], forming monomeric [12c], dimeric [12f], tetrameric [12g, 12h] and polymeric [12] structures, some of which form 1D and 2D structures through hydrogen bonding.

In compound **2**, the polyfunctional ligand **L2** coordinates the metal only monodentately and does not chelate and/or bridge the two cobalt atoms, even though the lattice **L2** ligand and the $[Co(H_2O)_6\}]^{2+}$ cation participate in forming the crystal structure. Generally, the **L2** ligand tends to chelate and/or bridge the metal atoms, and therefore the size of the ionic radii of the metal has an effect. In addition to the Co^{2+} ion (ionic radius 0.745 Å [19]), the **L2** also binds the hexacoordinate Mg^{2+} ion (ionic radius 0.72 Å [19]) in a monodentate fashion [13]. With hexacoordinate Ni^{2+} (ionic radius 0.69 Å [19]) and Zn^{2+} ions (ionic radius 0.74 Å [19]), the **L2** ligand coordinates metals in a monodentate manner, but also bridges them to the hexacoordinate Na^{+} ion (ionic radius 1.02 Å [19]), forming polymeric chains [14]. In complex **3** with hexacoordinate Mn^{2+} (ionic radius 0.83 Å [19]), and with octa- and nonacoordinate

Sr^{2+} (ionic radii 1.26 and 1.31 Å, respectively [19]), and octacoordinate Ba^{2+} ions (ionic radius 1.42 Å [19]), the **L2** ligand both chelates and bridges the metal atoms, and forms a dimeric structure with Mn^{2+} and also polymeric structures with Sr^{2+} and Ba^{2+} ions [13]. In consequence, the **L2** ligand both chelates and bridges metal atoms with ionic radii > 0.80 Å, but otherwise it acts as a monodentate or bidentate ligand without forming chelate rings. All metal complexes of the **L2** ligand form 2D structures through the hydrogen bonding of crystal water and coordinated water. In addition, the other diester derivatives, where the ester group is smaller, form also 1D structures through hydrogen bonding [12f].

Compound **4** and other geminal bisphosphonates, where the hydrophobic groups are attached to the middle carbon atom between the two phosphonate groups, form 0–3D structures some of which are extended to 3D structures through hydrogen bonding [6c–6e, 7c–7f, 8b–8e, 8g, 18c–18e]. In addition, π–π stacking interactions may occur in the case of risedronate [18c–18e].

In conclusion, the flexible and hydrophilic clodronic acid ligand **L1** is able to form a 3D hydrogen-bonded network. As mentioned before [14], the bulky organic groups attached to the phosphonate oxygen atoms, for example the diester groups in ligand **L2**, lead to 2D dense packing modes without solvent-accessible voids. The monoester derivatives, in turn, are capable of forming a 3D hydrogen bond network. If the hydrophobic groups are located in the middle carbon chain between the phosphonate groups, as in **L3**, the 3D hydrogen bond network may be formed. This indicates that the designing of new 3D porous materials from metal bisphosphonates could also be focused on the addition of chains with suitable coordinating groups to the middle carbon atom. In all bisphosphonate structures, the additional lattice ligands or guest molecules, e.g. water and acetone etc., play a significant role in determining the structural properties and achieving more open structures. The general problem is the easy removability of the guest molecules without breaking the crystal structure, to open the voids for other molecules entering the structure in applications. More unusual are the additional lattice ligands, e.g. **L2**, in the nickel [14], zinc [14], and cobalt (**2**) complexes of **L2**, which do not participate in coordination to the metal atoms.

Spectroscopic Properties

The assignments of the cobalt, manganese and copper complexes **1**–**4** are based on earlier results, on published values for similar compounds and on IR spectroscopic tables [3a, 3b, 12–14]. The characteristic signals for complex **1** appeared in the region 1636–776 cm^{-1}, for compounds **2** and **3** the characteristic signals were observed in the range 1735–685 cm^{-1}, and for compound **4** in the range 3150–705 cm^{-1}. The stretching frequency of the O–H bonds of the water cluster pattern in complex **1** was observed as a broad band at around 3420 cm^{-1}. The same frequencies of ice appear at 3220 cm^{-1} and of liquid water at 3490 cm^{-1} and 3280 cm^{-1} [5c]. In addition, broad bands of $\nu(H_2O)$ around 3410–3520 cm^{-1} and weaker absorptions of δ(H–O–H) in the region 1630–1640 cm^{-1} were observed in the spectra of compounds **2**–**4**. Absorptions due to the bis(phosphonic) acid framework of **1**–**4** were found at 1295–970 cm^{-1}, which could be attributed to the stretching vibrations of the phosphonate PO_3 groups, and signals at 860–760 cm^{-1} were assigned to asymmetric and symmetric ν(P–C–P) vibrations. In compounds **1**–**3**, the asymmetric and symmetric $\nu(CCl_2)$ vibrations appeared at 805–685cm^{-1}.

The difference between the IR spectra of the metal complex of **L1** (**1**), and the metal complexes of **L2** (**2**, **3**), is that the ν(P=O) absorption is shifted approximately 150 cm^{-1} to higher wavenumbers in the spectra of compounds **2** and **3**, due to the benzoyl groups attached to the phosphonate groups. In addition, the spectra of compounds **2** and **3** showed other bands resulting from the benzoyl groups of the ligand **L2**. The absorptions of ν(C=O) appeared at 1730 cm^{-1}, and the absorptions of ν(C–O) appeared at 1270 cm^{-1} and 1135 cm^{-1}. The aromatic ring ν(C=C) vibrations occurred at 1605 cm^{-1}, 1590 cm^{-1}, 1495 cm^{-1}, and 1455 cm^{-1} and the stretching vibrations of the ring C–H bonds appeared as a series of bands in the 3100–2800 cm^{-1} region. Absorptions of the monosubstituted aromatic ring, resulting from out-of-plane C–H vibrations, appeared at ca. 750 cm^{-1} and 700 cm^{-1}. In addition, in the spectrum of pyridyl compound **4**, the characteristic broad bands of the pyridine ring are in the same region than the CH_2 and PO_3 stretching vibrations, which makes the reading of the spectrum difficult. The spectrum of complex **4** shows aromatic C–H stretching vibrations as a broad band at 3150–3010 cm^{-1}, and as a weak overtone and combined bands at 2200–2000 cm^{-1}. The signals in the latter region can also result from protonated phosphonate groups. The C=C and C=N stretching vibrations give rise to a band at 1640–1360 cm^{-1} and a strong broad band was observed at 1140–910 cm^{-1}.

Thermogravimetric Analyses

The TGA diagram for compound **1** shows three overlapped weight loss steps at about 50–160 °C, 160–350 °C, and 350–800 °C, which are attributable to the release of lattice water, coordinated water and chlorine atoms. The TGA diagram for compound **2**, in turn, shows three overlapped weight loss steps at about 50–200 °C, 200–250 °C, and 250–800 °C, which are attributable to the release of aqua ligands, chlorine atoms and three benzoyl groups. The total weight losses of 47.9 % for **1** and 55.4 % for **2** are in good agreement with the theoretical values of 48.3 % and 55.1 %, respectively.

The TGA diagram for complex **3** indicates that it is stable up to 100 °C, probably due to the structure-strengthening chelate rings and the lack of crystal water. The TGA diagram exhibit three overlapped weight loss steps at about 100–230 °C, 230–300 °C, 300–800 °C attributable to the release of aqua ligands, chlorine atoms, and finally, two benzoyl groups. The total weight loss of 57.0 % for **3** is in good agreement with the calculated value of 59.8 %.

The TGA diagram for complex **4** indicates that the compound is stable up to 150 °C. The TGA diagram shows four partly overlapped weight loss steps at about 150–200 °C, 200–245 °C, 245–455 °C, and 455–800 °C, which are attributable

Zeitschrift für anorganische und allgemeine Chemie ZAAC Journal of Inorganic and General Chemistry

to the release of crystal water, coordinated water, hydroxyl groups, and pyridyl groups. The total weight loss of 42.3 % for **4** is in good agreement with the calculated value of 41.8 %.

The identifiable phases of the black final multiphase products of compounds **1**–**2** and **4** could not be identified definitely by means of powder X-ray diffractometry, since the cobalt and copper complexes create strong noise due to the fluorescence. The calculable final products of compounds **1**–**2** and **4** are $Co(PO_3)_2$, $Co_2C_9OH_5(PO_3)_4$ and $CuC_2(PO_3)_4$, respectively. The identifiable phase of the final black crystalline and multiphase product of complex **3** was identified to be manganese phosphate $Mn(P_4O_{11})$, whereas the calculable final product is $MnC(PO_3)_2$.

Conclusions

Four new metal complexes of unique and modified bis(phosphonate) ligands (**1**–**4**) were synthesised and characterised. These new metal bis(phosphonates) form 2D and 3D structures through extensive hydrogen bond network, and thus the additional lattice ligands play a significant role in determining the structural properties. Present and earlier studies [14] show how monomeric and dimeric metal clodronates form a 3D hydrogen bond network around them. In cobalt clodronate (**1**), the 2D tape-like water cluster patterns formed by hydrogen bonds between the lattice water and coordinated water molecules place themselves between the dinuclear units. 3D hydrogen bonding interactions occur when the phosphonate oxygen atoms serve as hydrogen-bond acceptors. The 3D hydrogen bond network can also be seen in copper risedronate (**4**), where the protonated pyridyl nitrogen atoms and hydroxyl group between the phosphonate groups participate in hydrogen bonding in addition to the coordinated and crystal water and phosphonate oxygen atoms. Additionally, the pyridine rings form intermolecular π–π stacking interactions with the adjacent rings. The cobalt and manganese complexes of **L2** (**2** and **3**), show the typical 2D arrangement of the units through hydrogen bonding. Interesting here is the effect of the size of the metal ion in structure formation. Thus far, the **L2** ligand both chelates and bridges metal atoms with ionic radii > 0.80 Å, but otherwise it acts as a monodentate or bidentate ligand without forming chelate rings.

In the present study we demonstrated the effects of metal and different kind of substituted groups in bis(phosphonate) ligands on the structure formation of bis(phosphonates), on IR spectroscopic frequencies and on thermogravimetric measurements. The water clusters of complex **1** and lattice water in compounds **2** and **4** were found and refined during the structural refinement process. They were experimentally observed and described, which might enhance our understanding of the properties of liquid water in terms of its space-filling role in crystal structures. In addition, this study provides important information for research into bis(phosphonates) as pharmaceutical products, since the ionic radiuses of the first row transition metals are similar to the ionic radii of the alkaline earth metals. The investigation of the coordination properties of the modified bis(phosphonates), drugs and possible prodrugs, toward divalent metals, would be helpful in understanding the adsorption of the drug onto human bone and the binding properties toward metal cations in the human body. The scaling of the syntheses and studies of the complexing properties of other bis(phosphonates) are now in progress.

Experimental Section

General Procedures

All reagents used for the synthesis and characterisation of compounds **1**–**4** were of analytical reagent grade. The synthesis and characterisation of *P,P'*-dibenzoyl-dichloromethylenebis(phosphonate) disodium salt, $Na_2Cl_2C[PO_3(COC_6H_5)]_2$ (Na_2**L2**), were reported earlier [11a].

Table 4. Crystal data for compounds **1**–**4**.

	1	**2**	**3**	**4**
Empirical formula	$CH_{22}Cl_2Co_2O_{17}P_2$	$C_{30}H_{46}Cl_4Co_2O_{29}P_4$	$C_{30}H_{32}Cl_4Mn_2O_{22}P_4$	$C_{14}H_{28}CuN_2O_{18}P_4$
Formula weight	556.89	1254.21	1120.12	699.80
Temperature /K	100(2)	100(2)	100(2)	100(2)
Crystal system	Monoclinic	Triclinic	Monoclinic	Triclinic
Space group	$P2_1/c$	$P1$	$P2_1/n$	$P\bar{1}$
a /Å	8.4768(1)	7.0225(2)	7.5320(1)	7.6516(3)
b /Å	13.5729(2)	10.5820(4)	9.9230(2)	8.5823(5)
c /Å	15.1066(2)	16.9475(6)	28.5510(5)	10.2829(5)
α /°	90	88.204(2)	90	65.908(2)
β /°	91.8180(9)	82.207(2)	92.177(1)	84.953(3)
γ /°	90	72.646(2)	90	78.852(3)
V /Å^3	1737.21(4)	1190.92(7)	2132.36(6)	604.78(5)
Z	4	1	2	1
ρ_{calc} /g·cm^{-3}	2.129	1.749	1.745	1.919
μ(Mo-K_α) /mm^{-1}	2.481	1.149	1.076	1.260
GOF on F^2	1.079	1.028	1.043	1.091
R_{int}	0.0373	0.0289	0.0497	0.0542
R_1[a)] ($I \geq 2\sigma$)	0.0238	0.0302	0.0321	0.0331
wR_2[b)] ($I \geq 2\sigma$)	0.0548	0.0655	0.0675	0.0799

a) $R_1 = \Sigma\|F_o|-|F_c\|/\Sigma|F_o|$.b) $wR_2 = [\Sigma[w(F_o^2-F_c^2)^2]/\ \Sigma[w(F_o^2)^2]]^{1/2}$.

The risedronic acid was synthesised by the known method [21], but the product was changed into well crystallising disodium salt form $Na_2[(CH_2C_5H_5N)C(OH)(PO_3H)_2]$ (Na_2**L3**) by adjusting the pH with NaOH. Compound **1** was prepared by the gel crystallisation method, compounds **2** and **3** by the liquid crystallisation method and compound **4** by evaporation from the solution. In the present study, we are interested in the structural properties of compounds **1**–**4**, and therefore the characterisation analyses were performed by using crystals derived from additional crystallisations.

Single crystals of **1**–**4** were selected for structural determination with a Nonius Kappa CCD diffractometer. Elemental analyses for C and H were carried out with CarloErba 1106 and VarioMICRO V1.7.0 CHN Mode analysers, in which clodronate and EDTA served as standards. The percentage values of Co, Mn, and Cu were determined by using a Varian 220 atomic absorption spectrophotometer. The infrared spectra were recorded with a Nicolet Magna-IR™ spectrometer 750 by KBr pellet technique. Thermogravimetric analyses (TGA) were performed with a METTLER Toledo TGA/SDTA851^e for compounds **1**, **2** and **4** under a nitrogen gas flow at a heating rate of 5 °C·min^{-1} from 25 °C to 800 °C, and from 25 °C to 900 °C for compound **3**. Powder X-ray diffraction (XRD) data for the final products of TG analyses were collected with a Bruker Advance D8 diffractometer by using Cu-K_α radiation (λ = 1.5406 Å) in the 2θ range of 5–100° with a step size of 0.05° and a counting time of 3 s per step.

Syntheses

[Co_2{$Cl_2C(PO_3)_2$}$(H_2O)_7$·$4H_2O$] (1): A solution of **L1** in water (0.087 mmol, 0.9 mL, pH 3.45) was mixed with TMOS (0.1 mL). The concentrated solution of $Co(NO_3)_2$·$6H_2O$ in water (0.006 mol, 1.0 mL, pH 2.70) was placed above the gel (pH 3.51). After two weeks it was replaced with acetone (1.0 mL). Pale red block-like crystals formed on the surface of the gel (pH 2.42) within a month after the addition of the acetone. $CH_{22}Cl_2Co_2O_{17}P_2$ (556.89): calcd. C 2.16; H 3.98; Co 21.16 %; found C 2.09; H 4.05; Co 20.94 %. **IR** (KBr): $\tilde{\nu}$ = 1636 (m, d_{P-O}), 1130 (vs, $\nu_{P=O}$), 1018 (s, ν_{P-O}), 967 (m, ν_{P-O}), 889 (m, ν_{P-C-P}), 776 (m, ν_{P-C-P}), 770 (sh, ν_{C-Cl}) cm^{-1}.

[Co{$Cl_2C(PO_2O(C(O)C_6H_5))_2(H_2O)_5$}·$2H_2O${$Cl_2C(PO_2O(C(O)$-$C_6H_5))_2$}}{$Co(H_2O)_6$}] (2): Solutions of **L2** in water (0.030 mmol, 1 mL, pH 3.74) and of $Co(NO_3)_2$·$6H_2O$ in water (0.030 mmol, 1 mL, pH 4.49) were mixed with acetone (1 mL). The solution (pH 3.30) was allowed to stand cold and pale red plate-like crystals formed after four days (pH 3.22). $C_{30}H_{46}Cl_4Co_2O_{29}P_4$ (1254.21): calcd. C 28.73; H 3.70; Co 9.40 %; found C 28.56; H 3.71; Co 9.40 %. **IR** (KBr): $\tilde{\nu}$ = 1729 and 1711 (m,$\nu_{C=O}$), 1604 (m, $\nu_{C=C}$), 1586 (w, $\nu_{C=C}$), 1497 (w, $\nu_{C=C}$), 1456 (m, $\nu_{C=C}$), 1272 (s, $\nu_{P=O}$, ν_{C-O}), 1183 (m, ν_{C-O-P}), 1135 (m, ν_{C-O}), 1104 (m, ν_{C-C}), 1077 (m, ν_{P-O}), 1064 (m, ν_{P-O}), 1029 (m, ν_{P-O-C}), 1004 (w, ν_{P-O-C}), 843 (m, ν_{P-C-P}), 774 (m, ν_{P-C-P}, ν_{C-H}, ν_{C-Cl}), 703 (s, ν_{C-H}), 685 (m, ν_{C-Cl}) cm^{-1}.

[Mn{$[Cl_2C(PO_2O(C(O)C_6H_5))_2](H_2O)_3$}] (3): Solutions of **L2** in water (0.030 mmol, 1 mL, pH 3.75) and of $MnCl_2$·$4H_2O$ in water (0.030 mmol, 1 mL, pH 4.94) were mixed and acetone (1 mL) was added. The solution (pH 3.51) was allowed to stand cold and colourless block-like crystals formed after one day (pH 3.14). $C_{30}H_{32}Cl_4Mn_2O_{22}P_4$ (1120.12): calcd. C 32.21; H 2.89; Mn 9.83 %; found: C 32.33; H 2.80; Mn 9.78 %. **IR** (KBr): $\tilde{\nu}$ = 1735 and 1720m (m, $\nu_{C=O}$), 1605 (m, $\nu_{C=C}$), 1590 (w, $\nu_{C=C}$), 1496 (w, $\nu_{C=C}$), 1457 (m, $\nu_{C=C}$), 1294 (s, $\nu_{P=O}$), 1267 (s, ν_{C-O}), 1179 (w, ν_{C-O-P}), 1134 (m, ν_{C-O}), 1101 (m, ν_{C-C}), 1083 (m, ν_{P-O}), 1067 (s, ν_{P-O}), 1028 (m, ν_{P-O-C}), 1000 (vw, ν_{P-O-C}), 859 (m, ν_{P-C-P}), 805 (w, ν_{C-Cl}), 777 (m, ν_{P-C-P}), 765 (m, ν_{C-H}), 708 (s, ν_{C-H}), 687 (m, ν_{C-Cl}) cm^{-1}.

[Cu{$(CH_2C_5H_5N)C(OH)(PO_3H)_2$}$_2$·$4H_2O$] (4): A solution of **L3** in water (0.018 mmol, 0.5 mL, pH 4.4) was mixed with a solution of $Cu(NO_3)_2$·$2,5H_2O$ in water (0.018 mol, 0.5 mL, pH 4.4). Pale blue block-like crystals formed within two months (pH 4.0).

Table 5. Selected bond lengths /Å and angles /° for compounds **1**–**4**.

	1	2	3	4
P1–O2		1.473(2)	1.4720(14)	
P1–O1		1.488(2)	1.491(2)	1.527(2)
P1–O3		1.641(2)	1.6224(14)	1.557(2)
P1–O4				1.500(2)
P2–O6		1.493(2)	1.478(2)	1.568(2)
P2–O5		1.482(2)	1.479(2)	1.498(2)
P2–O7		1.630(2)	1.632(2)	
P2–O2				1.522(2)
P1B–O2B		1.478(2)		
P1B–O1B		1.482(2)		
P1B–O3B		1.649(2)		
P2B–O6B		1.477(2)		
P2B–O5B		1.484(2)		
P2B–O7B		1.654(2)		
P5–O9	1.5125(11)			
P5–O5	1.5221(11)			
P5–O10	1.5223(11)			
P6–O8	1.5088(11)			
P6–O4	1.5220(11)			
P6–O7	1.5336(11)			
P1–C1		1.861(3)	1.850(2)	1.848(2)
P2–C1		1.848(3)	1.856(2)	1.840(2)
P1B–C1B		1.855(3)		
P2B–C1B		1.860(3)		
P5–C1		1.856(2)		
P6–C1		1.850(2)		
O2–P1–C1		109.94(14)	108.93(9)	
O1–P1–C1		105.63(13)	107.67(9)	105.40(9)
O3–P1–C1		97.16(13)	96.44(8)	104.22(9)
O4–P1–C1				109.60(9)
O6–P2–C1		108.06(14)	108.78(9)	105.64(9)
O5–P2–C1		108.76(13)	106.46(9)	110.75(9)
O7–P2–C1		99.27(13)	97.99(8)	
O2–P2–C1				105.52(9)
O2B–P1B–C1B		107.34(13)		
O1B–P1B–C1B		108.33(13)		
O3B–P1B–C1B		99.80(12)		
O6B–P2B–C1B		109.44(14)		
O5B–P2B–C1B		107.39(14)		
O7B–P2B–C1B		96.24(13)		
O9–P5–C1	106.82(7)			
O5–P5–C1	106.05(7)			
O10–P5–C1	103.15(7)			
O8–P6–C1	106.74(7)			
O4–P6–C1	104.13(7)			
O7–P6–C1	105.62(7)			
P1–C1–P2		109.1(2)	109.69(10)	109.87(10)
P1B–C1B–P2B		108.8 (2)		
P5–C1–P6	115.38(8)			

$C_{14}H_{28}CuN_2O_{18}P_4$ (699.80): calcd. C 24.03; H 4.03; N 4.00 Cu 9.08 %; found C 23.89; H 3.92; N 4.00; Cu 8.91 %. **IR** (KBr): $\tilde{\nu}$ = 1123 (vs, $\nu_{P=O}$), 1061 (vs, ν_{PO3}), 978 (s, ν_{P-O}), 817 (m, ν_{P-C-P}), 762 (m, ν_{P-C-P}) cm^{-1}.

X-ray Crystallographic Study

Crystals of **1**–**4** were immersed in cryo-oil, mounted in a Nylon loop, and measured at a temperature of 100 K. The X-ray diffraction data were collected by means of a Nonius KappaCCD diffractometer using Mo-K_α radiation (λ = 0.71073 Å). The Denzo-Scalepack [22] program package was used for cell refinements and data reductions. The structures were solved by direct methods with SHELXS-97 [23] for compound **1** and with SIR2004 [24] for complexes **2**–**4**, with a WinGX [25] graphical user interface. A semi-empirical absorption correction (compounds **1**–**3**: SADABS [26], compound **4**: SORTAV [27]) was applied to all data. Structural refinements were carried out using SHELXL-97 [23]. Despite a rather large Flack parameter [0.243(9)] in compound **2**, the introduction of a racemic twin component did not improve the result, and the twin component was not used in the final refinement. All water hydrogen atoms in structure **1** were located on the difference Fourier map but were repositioned geometrically and constrained to ride on their parent atom, with U_{iso} = 1.5. In complexes **2**–**4** all of the water hydrogen atoms (and all of the NH and OH hydrogen atoms in complex **4**) were located on the difference Fourier map and constrained to ride on their parent atom, with U_{iso} = 1.5. Other hydrogen atoms in compounds **2**–**4** were positioned geometrically and were also constrained to ride on their parent atoms, with C–H = 0.95–0.99 Å and $U_{iso} = 1.2 \cdot U_{eq}$ (parent atom). The crystallographic details are summarised in Table 4 and selected bond lengths and angles are shown in Table 5.

Crystallographic data for the structures have been deposited with the Cambridge Crystallographic Data Centre, 12 Union Road, Cambridge CB21EZ. Copies of the data can be obtained free of charge on quoting the depository numbers CCDC-752487 (compound **1**), CCDC-752488 (compound **2**), CCDC-752489 (compound **3**), and CCDC-752490 (compound **4**). (Fax: +44-1223-336-033; E-Mail: deposit@ccdc.cam.ac.uk).

Supporting Information (see footnote on the first page of this article): IR spectra, TGA curves and hydrogen bond tables for compounds **1**–**4**.

Acknowledgement

We would like to thank *Tarja Virrantalo* for her assistance (Dept. Chem., Univ. Joensuu).

References

[1] a) A. Clearfield, in: *Progress in Inorganic Chemistry: Metal-Phosphonate Chemistry* (Ed.: K. D. Karlin), John Wiley & Sons, New York **1998**, pp. 373–510; b) A. Clearfield, *Dalton Trans.* **2008**, 6089–6102; c) L. Öhrström,K. Larsson, *Molecule-Based Materials – The Structural Network Approach*, Elsevier, Amsterdam **2005**, pp. 19–38; d) K. M. Fromm, *Coord. Chem. Rev.* **2008**, *252*, 856–885.

[2] a) H.-H. Song, L.-M. Zheng, Z. Wang, C.-H. Yan, X.-Q. Xin, *Inorg. Chem.* **2001**, *40*, 5024–5029; b) S. Bauer, H. Müller, T. Bein, N. Stock, *Inorg. Chem.* **2005**, *44*, 9464–9470; c) H. G. Harvey, S. J. Teat, M. P. Attfield, *J. Mater. Chem.* **2000**, *10*, 2632–2633; d) C. V. K. Sharma, A. Clearfield, *J. Am. Chem. Soc.* **2000**, *122*, 4394–4402; e) K. Barthelet, D. Riou, G. Férey, *Solid State Sci.* **2002**, *4*, 841–844; f) K. Barthelet, C. Merlier, C. Serre, M. Riou-Cavellec, D. Riou, G. Férey, *J. Mater. Chem.* **2002**, *12*, 1132–1137.

[3] a) M. Kontturi, S. Kunnas-Hiltunen, J. J. Vepsäläinen, M. Ahlgrén, *Solid State Sci.* **2006**, *8*, 1098–1102; b) M. Kontturi, E. Laurila, R. Mattsson, S. Peräniemi, J. J. Vepsäläinen, M. Ahlgrén, *Inorg. Chem.* **2005**, *44*, 2400–2406; c) C. Serre, G. Férey, *J. Mater. Chem.* **2002**, *12*, 2367–2369; d) Z.-G. Sun, L.-Y. Cui, Z.-M. Liu, L. Meng, H. Chen, D.-P. Dong, L.-C. Zhang, Z.-M. Zhu, W.-S. You, *Inorg. Chem. Commun.* **2006**, *9*, 999–1001; e) P. Yin, L.-M. Zheng, S. Gao, X.-Q. Xin, *Chem. Commun.* **2001**, 2346–2347; f) J. Liang, K. H. Shimizu, *Inorg. Chem.* **2007**, *46*, 10449–10451; g) R. Fu, S. Hu, H. Zhang, L. Wang, X. Wu, *Inorg. Chem. Commun.* **2005**, *8*, 912–915.

[4] a) P. Yin, Y. Peng, L.-M. Zheng, S. Gao, X.-Q. Xin, *Eur. J. Inorg. Chem.* **2003**, 726–730; b) H.-H. Song, P. Yin, L.-M. Zheng, J. D. Korp, A. J. Jacobson, S. Gao, X.-Q. Xin, *J. Chem. Soc., Dalton Trans.* **2002**, 2752–2759; c) D.-K. Cao, Y.-Z. Li, L.-M. Zheng, *Inorg. Chem.* **2007**, *46*, 7571–7578; d) H. G. Harvey, M. P. Attfield, *Chem. Mater.* **2004**, *16*, 199–209.

[5] a) L. Infantes, S. Motherwell, *CrystEngComm* **2002**, *4*, 454–461; b) L. Infantes, J. Chisholm, S. Motherwell, *CrystEngComm* **2003**, *5*, 480–486; c) D. Eisenberg,W. Kauzmann, *The Structure and Properties of Water*, Oxford University Press, Oxford **1969**; d) K. Raghuraman, K. K. Katti, L. J. Barbour, N. Pillarsetty, C. L. Barnes, K. V. Katti, *J. Am. Chem. Soc.* **2003**, *125*, 6955–6961; e) R. Ludwig, *Angew. Chem. Int. Ed.* **2001**, *40*, 1808–1827; f) S. K. Ghosh, P. K. Bharadwaj, *Inorg. Chem.* **2004**, *43*, 6887–6889; g) S. K. Ghosh, P. K. Bharadwaj, *Eur. J. Inorg. Chem.* **2005**, 4880–4885; h) S. K. Ghosh, P. K. Bharadwaj, *Inorg. Chim. Acta* **2006**, *359*, 1685–1689; i) S. K. Ghosh, P. K. Bharadwaj, *Eur. J. Inorg. Chem.* **2006**, 1341–1344.

[6] a) R. C. Finn, R. S. Rarig Jr., J. Zubieta, *Inorg. Chem.* **2002**, *41*, 2109–2123; b) R. C. Finn, J. Zubieta, *Inorg. Chem.* **2001**, *40*, 2466–2467; c) H.-H. Song, L.-M. Zheng, C.-H. Lin, S.-L. Wang, X.-Q. Xin, S. Gao, *Chem. Mater.* **1999**, *11*, 2382–2388; d) H.-H. Song, L.-M. Zheng, G. Zhu, Z. Shi, S. Feng, S. Gao, Z. Hu, X.-Q. Xin, *J. Solid State Chem.* **2002**, *164*, 367–373; e) H.-H. Song, L.-M. Zheng, Y.-J. Liu, X.-Q. Xin, A. J. Jacobson, S. Decurtins, *J. Chem. Soc., Dalton Trans.* **2001**, 3274–3278.

[7] a) D.-K. Cao, S. Gao, L.-M. Zheng, *J. Solid State Chem.* **2004**, *177*, 2311–2315; b) R. C. Finn, J. Zubieta, *J. Chem. Soc., Dalton Trans.* **2000**, 1821–1823; c) L.-M. Zheng, S. Gao, H.-H. Song, S. Decurtins, A. J. Jacobson, X.-Q. Xin, *Chem. Mater.* **2002**, *14*, 3143–3147; d) L.-M. Zheng, H.-H. Song, C.-Y. Duan, X.-Q. Xin, *Inorg. Chem.* **1999**, *38*, 5061–5066; e) P. Yin, Y. Peng, L.-M. Zheng, S. Gao, X.-Q. Xin, *Eur. J. Inorg. Chem.* **2003**, 726–730; f) X.-Y. Yi, L.-M. Zheng, W. Xu, S. Feng, *Inorg. Chem.* **2003**, *42*, 2827–2829.

[8] a) R. C. Finn, R. Lam, J. E. Greedan, J. Zubieta, *Inorg. Chem.* **2001**, *40*, 3745–3754; b) L.-M. Zheng, H.-H. Song, C.-H. Lin, S.-L. Wang, Z. Hu, Z. Yu, X.-Q. Xin, *Inorg. Chem.* **1999**, *38*, 4618–4619; c) P. Yin, L.-M. Zheng, S. Gao, X.-Q. Xin, *Chem. Commun.* **2001**, 2346–2347; d) P. Yin, Y. Peng, L.-M. Zheng, S. Gao, X.-Q. Xin, *Eur. J. Inorg. Chem.* **2003**, 726–730; e) H.-H. Song, P. Yin, L.-M. Zheng, J. Korp, A. J. Jacobson, S. Gao, X.-Q. Xin, *J. Chem. Soc., Dalton Trans.* **2002**, 2752–2759; f) A. Distler, D. L. Lohse, S. C. Sevov, *J. Chem. Soc., Dalton Trans.* **1999**, 1805–1812; g) Y. Gong, W. Tang, W. Hou, Z. Zha, C. Hu, *Inorg. Chem.* **2006**, *45*, 4987–4995; h) K. Barthelet, M. Nogues, D. Riou, G. Férey, *Chem. Mater.* **2002**, *14*, 4910–4918; i) N. G. Armatas, D. G. Allis, A. Prosvirin, G. Carnutu, C. J. O'Connor, K. Dunbar, J. Zubieta, *Inorg. Chem.* **2008**, *47*, 832–854; j) R. Fu, S. Hu, X. Wu, *Cryst. Growth Des.* **2007**, *7*, 1134–1144; k) A. Clearfield, *J. Alloys Compd.* **2006**, *418*, 128–138; l) S. Konar, J. Zon, A. V. Prosvirin, K. R. Dunbar, A. Clearfield, *Inorg. Chem.* **2007**, *46*, 5229–5236; m) C. A. Merrill, A. K. Cheetham, *Inorg. Chem.*

2007, *46*, 278–284; n) C. A. Merrill, A. K. Cheetham, *Inorg. Chem.* **2005**, *44*, 5273–5277; o) A. K. Cheetham, G. Férey, T. Loiseau, *Angew. Chem. Int. Ed.* **1999**, *38*, 3268–3292.

[9] a) Z. Wang, J. M. Heising, A. Clearfield, *J. Am. Chem. Soc.* **2003**, *125*, 10375–10383; b) A. Clearfield, *Chem. Mater.* **1998**, *10*, 2801–2810; c) Z. Yuan, W. Clegg, M. P. Attfield, *J. Solid State Chem.* **2006**, *179*, 1739–1749; d) M. P. Attfield, C. Mendieta-Tan, Z. Yuan, W. Clegg, *Solid State Sci.* **2008**, *10*, 1124–1131.

[10] a) R. G. G. Russell, *Ann. N. Y. Acad. Sci.* **2006**, *1068*, 367–401; b) J. H. Lin, *Bone.* **1996**, *18*, 75–85; c) R. Hannuniemi, L. Laurén, H. Puolijoki, *Drugs Today* **1991**, *27*, 375–390.

[11] a) M. Ahlmark, J. Vepsäläinen, H. Taipale, R. Niemi, T. Järvinen, *J. Med. Chem.* **1998**, *42*, 1473–1476; b) M. Ahlmark, J. J. Vepsäläinen, *Tetrahedron* **2000**, *56*, 5213–5219; c) J. Vepsäläinen, *Tetrahedron Lett.* **1999**, *40*, 8491–8493; d) J. Vepsäläinen, P. Vainiotalo, H. Nupponen, E. Pohjala, *Acta Chem. Scand.* **1997**, *51*, 932–937.

[12] a) J. Jokiniemi, S. Peräniemi, J. Vepsäläinen, M. Ahlgrén, *Acta Crystallogr., Sect. E* **2009**, *65*, m436–m437; b) J. Jokiniemi, J. Vepsäläinen, H. Nätkinniemi, S. Peräniemi, M. Ahlgrén, *CrystEngComm* **2009**, DOI: 10.1039/B907874F; c) J. Jokiniemi, E. Vuokila-Laine, S. Peräniemi, J. J. Vepsäläinen, M. Ahlgrén, *CrystEngComm* **2007**, *9*, 158–164; d) J. Jokiniemi, S. Peräniemi, J. Vepsäläinen, M. Ahlgrén, *Acta Crystallogr., Sect. C* **2009**, *65*, m165–m167; e) J. Jokiniemi, S. Peräniemi, J. J. Vepsäläinen, M. Ahlgrén, *CrystEngComm* **2008**, *10*, 1011–1017; f) M. Kontturi, E. Vuokila-Laine, S. Peräniemi, T. T. Pakkanen, J. J. Vepsäläinen, M. Ahlgrén, *J. Chem. Soc., Dalton Trans.* **2002**, 1969–1973; g) M. Kontturi, S. Peräniemi, J. J. Vepsäläinen, M. Ahlgrén, *Eur. J. Inorg. Chem.* **2004**, 2627–2631; h) M. Kontturi, S. Peräniemi, J. J. Vepsäläinen, M. Ahlgrén, *Polyhedron* **2005**, *24*, 305–309; i) M. Kontturi, S. Peräniemi, J. J. Vepsäläinen, M. Ahlgrén, *Acta Crystallogr., Sect. E* **2005**, *61*, m635–m637; j) J. Jokiniemi, J. Vepsäläinen, M. Ahlgrén, *Acta Crystallogr., Sect. E* **2009**, *65*, m600–m601; k) M. Kontturi, S. Peräniemi, J. J. Vepsäläinen, M. Ahlgrén, *Acta Crystallogr., Sect. E* **2004**, *60*, m1060–m1062.

[13] S. Kunnas-Hiltunen, M. Matilainen, J. Vepsäläinen, M. Ahlgrén, *Polyhedron* **2009**, *28*, 200–204.

[14] S. Kunnas-Hiltunen, M. Haukka, J. Vepsäläinen, M. Ahlgrén, *Eur. J. Inorg. Chem.* 355335–5345.

[15] a) G. Bonavia, C. Haushalter, C. J. O'Connor, J. Zubieta, *Inorg. Chem.* **1996**, *35*, 5603–5612; b) J. Salta, J. Zubieta, *Inorg. Chim. Acta* **1996**, *252*, 431–434.

[16] a) H. G. Harvey, S. J. Teat, C. C. Tang, L. M. Cranswick, M. P. Attfield, *Inorg. Chem.* **2003**, *42*, 2428–2429.

[17] a) P. van der Sluis, A. L. Spek, *Acta Crystallogr., Sect. A* **1990**, *46*, 194–201; b) A. L. Spek, *J. Appl. Crystallogr.* **2003**, *36*, 7–13; c) H. Küppers, F. Liebau, A. L. Spek, *J. Appl. Crystallogr.* **2006**, *39*, 338–346.

[18] a) W. L. Gossmann, S. R. Wilson, E. Oldfield, *Acta Crystallogr., Sect. C* **2003**, *59*, m33–m36; b) N. Redman-Furey, M. Dicks, A. Bigalow-Kern, R. T. Cambron, G. Lubey, C. Lester, D. Vaughn, *J. Pharm. Sci.* **2005**, *94*, 893–911; c) K. Stahl, J. Oddershede, H. Preikschat, E. Fischer, J. S. Bennekou, *Acta Crystallogr., Sect. C* **2006**, *62*, m112–m115; d) Z.-C. Zhang, S. Gao, L.-M. Zheng, *Dalton Trans.* **2007**, 4681–4684; e) J. Hu, J. Zhao, H. Hou, Y. Fan, *Inorg. Chem. Commun.* **2008**, *11*, 1110–1112.

[19] R. D. Shannon, *Acta Crystallogr., Sect. A* **1976**, *32*, 751–767.

[20] a) J. Kivikoski, J. M. Garcia-Ruiz, J. Vepsäläinen, F. Higes, E. Pohjala, J. Välisaari, *J. Phys. D: Appl. Phys.* **1993**, *26*, B172–B175; b) G. Socrates, *Infrared and Raman Characteristic Group Frequencies*, John Wiley & Sons, Chichester **2001**, pp. 229–240.

[21] a) G. R. Kieczykowski, R. B. Jobson, D. G. Melillo, D. F. Reinhold, V. J. Grenda, I. Shinkai, *J. Org. Chem.* **1995**, *60*, 8310–8312.

[22] Z. Otwinowski,W. Minor, in: *Methods in Enzymology, Volume 276, Macromolecular Crystallography, Part A* (Ed.: C. W. Carter, J. Sweet), Academic Press, New York, USA **1997**, pp. 307–326.

[23] G. M. Sheldrick, *Acta Crystallogr., Sect. A* **2008**, *64*, 112–122.

[24] M. C. Burla, M. Camalli, B. Carrozzini, G. L. Cascarano, C. Giacovazzo, G. Polidori, R. Spagna, *J. Appl. Crystallogr.* **2005**, *38*, 381–388.

[25] L. J. Farrugia, *J. Appl. Crystallogr.* **1999**, *32*, 837–838.

[26] Sheldrick, G. M. *SADABS* – Bruker Nonius Scaling and Absorption Correction, V 2.10, Bruker AXS, Inc., Madison, Wisconsin, USA, **2003**.

[27] R. H. Blessing, *Acta Crystallogr., Sect. A* **1995**, *51*, 33–38.

Received: December 9, 2009
Published Online: February 1, 2010

